Chapter

The Effect of Liquid Viscosity on the Rise Velocity of Taylor Bubbles in Small Diameter Bubble Column

Olumayowa T. Kajero, Mukhtar Abdulkadir, Lokman Abdulkareem and Barry James Azzopardi

Abstract

The rise velocity of Taylor bubbles in small diameter bubble column was measured via cross-correlation between two planes of time-averaged void fraction data obtained from the electrical capacitance tomography (ECT). This was subsequently compared with the rise velocity obtained from the high-speed camera, manual time series analysis and likewise empirical models. The inertia, viscous and gravitational forces were identified as forces, which could influence the rise velocity. Fluid flow analysis was carried out using slug Reynolds number, Froude number and inverse dimensionless viscosity, which are important dimensionless parameters influencing the rise velocity of Taylor bubbles in different liquid viscosities, with the parameters being functions of the fluid properties and column diameter. It was found that the Froude number decreases with an increase in viscosity with a variation in flow as superficial gas velocity increases with reduction in rise velocity. A dominant effect of viscous and gravitational forces over inertia forces was obtained, which showed an agreement with Stokes law, where drag force is directly proportional to viscosity. Hence, the drag force increases as viscosity increases ($5 < 100 < 1000 < 5000$ mPa s), leading to a decrease in the rise velocity of Taylor bubbles. It was concluded that the rise velocity of Taylor bubbles decreases with an increase in liquid viscosity and, on the other hand, increases with an increase in superficial gas velocity.

Keywords: structure velocity, cross-correlation, drag force, dimensionless number, electrical capacitance tomography

1. Introduction

Slug flow is characterized by Taylor bubbles, which has large pockets of bullet shaped bubbles occupying almost the entire cross-section of the column. The Taylor bubble is surrounded by a thin film of liquid, and below, it is the liquid slugs, which are agglomerate of small bubbles. Zukoski [1], Tomiyama et al. [2] and Mandal and Das [3] described the Taylor bubble length to exceed 1.5 times of the tube diameter or its diameter is greater than 60% of the tube diameter. The rise velocity of a single isolated Taylor bubble is dependent on inertia and drag forces [4]. A number of parameters affect the rise velocity of Taylor bubbles through a stagnant liquid; such

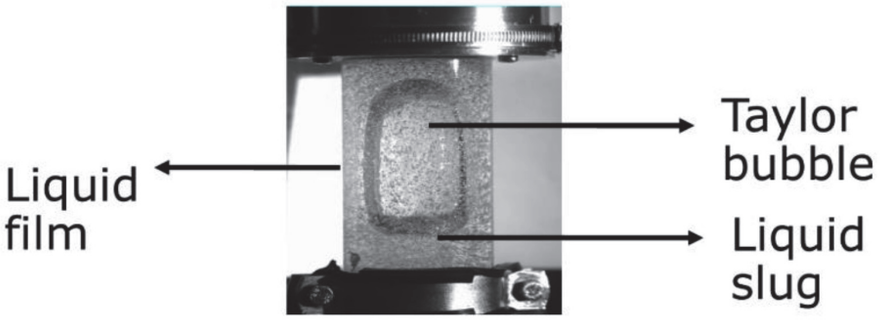

Figure 1.
A single Taylor bubble rising through a stagnant silicone oil liquid (viscosity, 1000 mPa s).

parameters include density of liquid, surface tension of liquid, liquid viscosity, acceleration due to gravity, diameter of bubbles etc. [5]. Mao and Dukler [6] explained that in a situation whereby the liquid is flowing, the rise velocity of a Taylor bubble must depend on the velocity of the liquid flowing upstream as well as the rise due to buoyancy. A typical example of bubble rising through a stagnant liquid as taken from a high-speed video camera (from the current study) is shown in **Figure 1**.

1.1 Background

The rise velocity of Taylor bubbles is otherwise known as structure velocity. It can also be defined as the velocity of periodic structures in the slug [7, 8]. Some researchers have carried out studies on the rise velocity of Taylor bubbles through stagnant liquid. Mao and Dukler [9] from their experimental results explained that for a wide range of viscosity and surface tension, the rise velocity can be expressed in terms of a constant Froude number.

$$Fr = \frac{U_N}{\sqrt{gD}} = constant \tag{1}$$

Hence, the rise velocity of Taylor bubble is given as:

$$U_N = Fr\sqrt{gD} \tag{2}$$

where g is the acceleration due to gravity and D is the diameter of the tube.

The rise velocity of Taylor bubbles in stagnant liquids was first studied by Dumitrescu [10] and Davies and Taylor [11] in which observed bubbles were of characteristics shape referred to as Dumitrescu or Taylor bubbles. Griffith and Wallis [12] eventually proposed the name as Taylor bubbles. Dumitrescu [10] carried out a study on the rise velocity of bubbles using water in a vertical tube and it was established both theoretically and experimentally that the bubble velocity was:

$$U_N = 0.35\sqrt{gD} \tag{3}$$

This is synonymous to the proposition of Mao and Dukler [9], where Froude's number is given as 0.35.

Dumitrescu [10] assumed that the bubble would have a spherical nose, solving simultaneously the flow around the bubble and the asymptotic film which eventually led to the bubble velocity [13] given as Eq. (3).

Davies and Taylor [11] gave the bubble velocity as:

$$U_N = 0.328\sqrt{gD} \tag{4}$$

after solving the problem using different assumptions.

Nicklin et al. [7] later postulated that the Davies and Taylor [11] solution was not unique but should tend to the limiting value given as:

$$U_N = 0.346\sqrt{gD} \tag{5}$$

Eqs. (3) and (4) proposed by Dumitrescu [10] and Davies and Taylor [11], respectively, assume that the Taylor bubble was obtained from a gas of zero density [13]. Neal [14] proposed that if the bubble density is significant, the bubble velocity is given as:

$$U_N = c\sqrt{gD\left(\frac{\Delta\rho}{\rho_L}\right)} \tag{6}$$

where c is approximately 0.35, $\Delta\rho = \rho_L - \rho_G$, ρ_L and ρ_G are the liquid and gas densities respectively.

Brown [15] from his experimental studies found that the solutions of Dumitrescu [10] and Davies and Taylor [11] were not suitable for high viscosity liquids, that they only describe the behaviour of gas bubbles in low viscosity liquids [13]. So, Brown [15] gave the bubble velocity as:

$$U_N = 0.35\sqrt{g(D - 2\delta_o)} \tag{7}$$

$$\text{where } \delta_o = \frac{D\sqrt{1 + N_{LB}} - D}{N_{LB}} \tag{8}$$

and

$$N_{LB} = \left(\frac{14.5\rho_L^2 D^3 g}{\mu_L^2}\right) \tag{9}$$

where N_{LB} is the liquid viscosity number and μ_L is the liquid viscosity.

Zukoski [1] proposed an expression for velocity of large bubbles in a closed horizontal pipe with large diameter (neglecting surface tension effects) given as:

$$U_N = 0.54\sqrt{gD} \tag{10}$$

where the Froude number is 0.54.

A correlation for the bubble rise velocity was proposed by Griffith and Wallis [12] based on the studies on vertical slug flow given as:

$$U_N = (U_{SG} + U_{SL}) + K_1.K_2\sqrt{gD} \tag{11}$$

where U_{SG} and U_{SL} are the superficial gas and liquid velocities respectively, and K_1 = 0.35.

They investigated the effect of different velocity profiles in the liquid slug by varying K_2 [16].

Nicklin et al. [7] from their vertical slug experiments proposed the rise velocity of a Taylor bubble in the liquid in a vertical tube as:

$$U_N = C_o(U_{SG} + U_{SL}) + U_o \tag{12}$$

where U_o is the translational velocity in a stagnant liquid or velocity of bubble propagating into stagnant liquid, given as:

$$U_o = 0.35\sqrt{gD} \tag{13}$$

where C_o is the distribution coefficient which is close to 1.2 for fully developed turbulent flow (low viscous liquid e.g. water) and close to 2 for laminar flow (high viscous liquid e.g. 1000 mPa s silicone oil) [7, 17–19].

From the experimental work reported by Sylvester [20], the rise velocity of Taylor bubble was presented as:

$$U_N = C_o(U_{SG} + U_{SL}) + C_1\left[\frac{gD(\rho_L - \rho_G)}{\rho_L}\right]^{1/2} \tag{14}$$

where D is the pipe diameter. They proposed C_o and C_1 to be 1.2 and 0.35, respectively.

From the experiment carried out by Bendiksen [21] in a vertical tube with flowing liquid, the distribution coefficient, C_o was obtained to be 1.2 for Reynold's number in the range 5000–110,000, i.e. low viscous liquid.

Nicklin et al. [7] interpreted their equation as:

Rise velocity of Taylor bubble (structure velocity) is equal to the velocity of the liquid at the tip of the bubble nose plus the rise velocity of bubble in a stagnant liquid (translational velocity).

Mao and Dukler [6] called this effective upstream velocity (rise velocity of Taylor bubble), the centreline velocity of the liquid.

White and Beadmore [22] carried out an experimental investigation on the rise velocity of Taylor bubbles through liquids in a vertical tube using three dimensionless parameters: Froude number, Fr, Eotvos number, E_o and Morton number, M_o. A recent review on vertical gas–liquid slug flow which highlights previous works on the rise velocity of Taylor bubbles is provided by Morgado et al. [23]. They discussed experimental, theoretical and numerical methods of investigating the rise velocity of Taylor bubbles, where the so-called numerical methods involve the use of empirical correlations. The limitations of these studies that have been addressed in the current study include (1) low range of liquid viscosities and more emphasis on low viscosities rather than high viscosities, (2) consideration of column or pipe diameter greater than 50 mm, (3) limited exploration of the effect of forces such as surface tension, inertia, gravitational and viscous forces acting on Taylor bubble, (4) limited exploration of the relationship between fluid dimensionless parameters and the Taylor bubble rise velocity, and (5) detailed comparison between different methods for obtaining the Taylor bubble rise velocity.

The rising Taylor bubble in a stagnant liquid as observed from the high-speed camera and ECT instrument 3D image (from current study) can be seen in **Figure 2**.

1.2 Fluid flow studies using dimensionless numbers

A significant number of dimensionless parameters have been identified to be of relevance in fluid flow studies. Examples of such include bond number, capillary number, drag coefficient, Froude number, inverse dimensionless viscosity, Reynolds number and Weber number to mention a few. In this study, the Reynolds

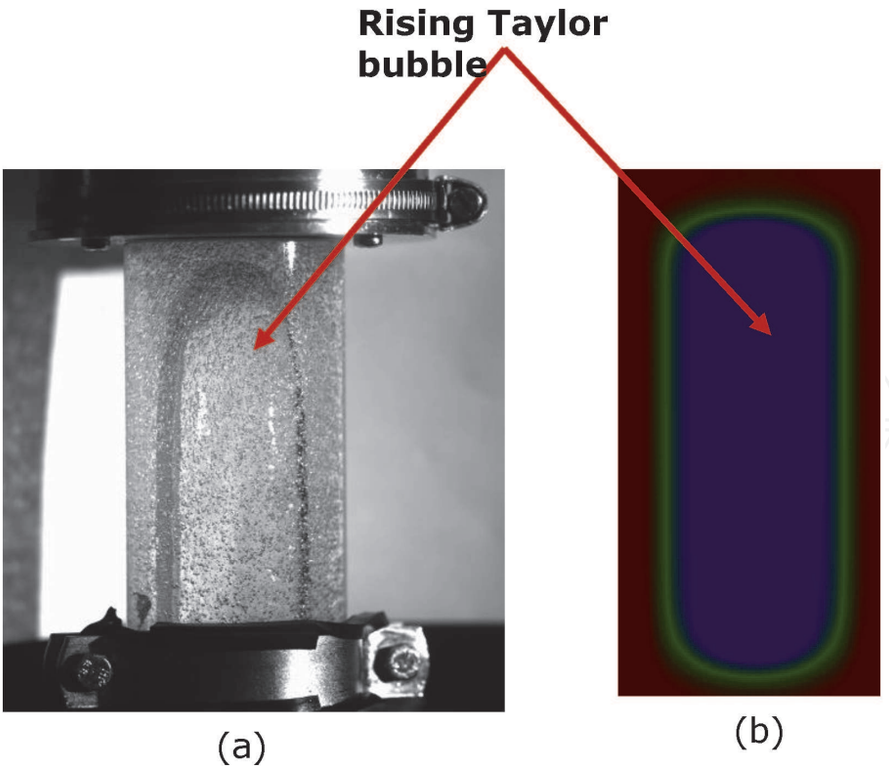

Figure 2.
Rising Taylor bubble from (a) high speed camera and (b) ECT instrument for 1000 mPa.s silicone oil at 0.361 m/s gas superficial velocity.

number, inverse dimensionless viscosity and Froude number were used to analyse the experimental results to clearly explain the effect of liquid viscosity on structure velocity.

1.2.1 Reynolds number, Re

The Reynolds number gives a measure of the ratio of inertia forces to viscous forces. Hence, it can be used to depict the competitive interplay between the effect of inertia forces and viscous forces [24].

$$\textit{Reynolds number}, \textit{Re} = \frac{\textit{Inertia forces}}{\textit{Viscous forces}} \tag{15}$$

Reynolds number can also be used to characterize flow regimes into laminar or turbulent flow. The occurrence of laminar flow is at low Reynolds number in which viscous forces dominate. This is characterized by smooth, constant fluid motion. Turbulent flow on the other hand is at high Reynolds numbers which is associated with chaotic eddies, vortices and other flow instabilities [25].

The slug Reynolds number which is the Reynolds number of the rising slug in the gas–liquid mixture [26–28] is expressed as:

$$Re = \frac{\rho U_M D}{\mu} \tag{16}$$

where μ = dynamic viscosity of the fluid, ρ = density of the fluid, D = diameter of column and U_M is the mixture velocity [26, 29].

1.2.2 Inverse dimensionless viscosity, N_f

According to Lu and Prosperetti [30], the inverse dimensionless viscosity is directly proportional to the fourth root of the Eotvos number raised to a power of three and inversely proportional to the fourth root of the Morton number. Morton number, M_o is used alongside with Eotvos number, E_o to characterize the shape of bubbles or drops moving in a surrounding fluid or continuous phase.

The inverse dimensionless viscosity is given as:

$$N_f = \left(\frac{E_o^3}{M_o}\right)^{1/4} \tag{17}$$

where Morton number is given as:

$$M_o = \frac{g\mu_L^4}{\rho_g \sigma_L^3} \tag{18}$$

Eotvos number is given as:

$$E_o = \frac{\rho g D}{\sigma_L} \tag{19}$$

1.2.3 Froude number

Apart from the effect of viscous force, gravitational force also affects the rise velocity of Taylor bubble through the liquid. Froude number is a dimensionless parameter which gives a relationship between inertia and gravitational forces. It describes different flow regimes of open channel flow as in the case of the bubble column in this study.

The slug Froude number [31] is given as Eq. (1). Llewellin et al. [5] called the Froude number a dimensionless velocity.

2. Experimental arrangements

The bubble column experimental set-up consists of a 50 mm internal diameter and 1.6 m long perspex column in a vertical orientation. At the bottom of the column is a single nozzle gas distributor through which gas is introduced into the column. A phantom high-speed camera was used to obtain the video of the gas–liquid flow in the column. A frame rate of 1000 pictures per second (pps) and exposure time of 100 μs was used. The geometry specified from the high-speed camera setting gives the image width by image height as 512 by 512 pixel.

Fitted midway to the column is the twin-planes electrical capacitance tomography (ECT) sensor with an interplanar spacing of 30 mm. The 8-electrode system consists of measurement and driven guard electrodes, which is connected to the electrical capacitance tomography processor box, TFLR 5000–20. This sensor electronics gives 28 measurements which are relayed to the computer where image reconstruction occurs, and the data are acquired and processed to obtain the liquid holdup (which is the fraction of liquid in the gas-liquid mixture). The void fraction otherwise known as gas holdup is hence obtained from this.

The ECT is located about 0.7 m above the nozzle, while the liquid level is located about 0.095 m above the ECT sensor. On injecting the gas, the gas flows into the

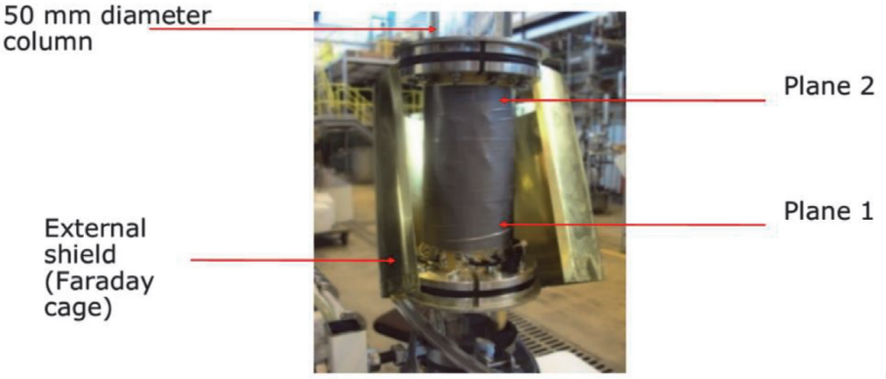

Figure 3.
The twin-plane ECT sensor used.

bubble column through the single nozzle gas injector with an orifice diameter of 6.8 mm. A range of silicone oil with viscosities 5, 100, 1000 and 5000 mPa s was used.

The liquid holdup obtained from the ECT was used to obtain the structure velocity (rise velocity of Taylor bubbles) via cross-correlation between two planes—plane 1 and plane 2 putting into consideration the distance between the two planes, 30 mm. The ECT sensor used is shown in **Figure 3**.

Further details of the experimental arrangements are given in Kajero et al. [32, 33].

3. Rise velocity of Taylor bubbles

In this study, the rise velocity of Taylor bubbles was obtained from ECT (via cross-correlation between signals from planes 1 and 2 as shown in **Figure 3**), manual time series analysis and the high-speed camera. This rise velocity of Taylor bubbles is also referred to as structure velocity which is from the Taylor bubble periodic structures velocity at real-time measurements.

3.1 Cross-correlation

Correlation is the measure of the degree of linear relationship between two variables. Cross-correlation is a statistical method of estimating the degree to which two variables (in this case, time series data sets) are correlated.

The structure velocity was computed from the cross-sectional time averaged void fraction data measured by the ECT for both planes 1 and 2. The cross-correlation between the signals obtained from the two planes gave the structure velocity.

Given two functions $\boldsymbol{x(t)}$ and $\boldsymbol{y(t)}$, the cross-correlation function, $\boldsymbol{R_{xy}(\tau)}$ between them is given as:

$$\boldsymbol{R_{xy}(\tau) = \lim_{T\to\infty} \frac{1}{T} \int_0^T x(t)y(t+\tau)d\tau} \tag{20}$$

The correlation coefficient function is expressed as:

$$\boldsymbol{\rho_{xy}(\tau) = \frac{C_{xy}(\tau)}{\sqrt{C_{xx}(0)C_{yy}(0)}} = \frac{R_{xy}(\tau) - \mu_x\mu_y}{\sqrt{\left(R_{xx}(0) - \mu_x^2\right)\left(R_{yy}(0) - \mu_y^2\right)}}} \tag{21}$$

where τ is the time delay, T is the record length (period), $C_{xy}(\tau)$ is the cross-covariance function, $C_{xx}(0)$ and $C_{yy}(0)$ are auto-covariance functions for x and y, respectively when time delay is zero, μ_x and μ_y are mean of the corresponding series, and $R_{xx}(0)$ and $R_{yy}(0)$ are the auto-correlation functions at a time delay of zero [34].

In this experimental work, the two functions $x(t)$ and $y(t)$ are time series data of planes 1 and 2, respectively.

The important parameters required for the computation of structure velocity using cross-correlation include:

a. Void fraction data for planes 1 and 2.

b. Number of data points.

c. Sampling frequency of data.

d. Distance between two planes (planes 1 and 2).

The time taken for the bubbles to travel between the two planes is calculated which then leads to the calculation of the structure velocity. This is done via an Excel Visual Basic Macro program used for the analysis of the time series data [35].

The time series, upstream and downstream with the corresponding correlation are shown in **Figure 4**. The time delay which is the time taken for the signal to travel between the two planes 1 and 2 is in the interval $-1 \leq \tau \leq 1$, where τ is the time delay.

Figure 4 indicates periodic structures of short slugs defined as advanced form of spherical cap bubbles gradually developing into clearly distinct slugs. These periodic structures are identified to be void waves in Taylor bubbles and liquid slugs in slug flow. Cross correlation of the time series data from the two axial locations can give

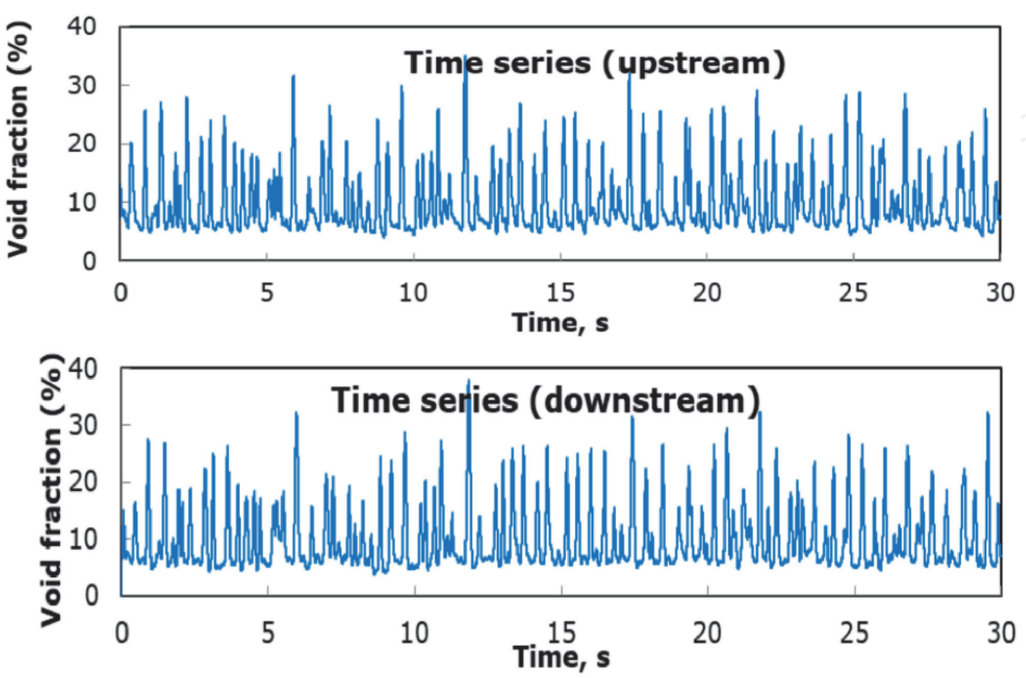

Figure 4.
Time series upstream and downstream for 5 mPa s silicone oil at a superficial gas velocity of 0.02 m/s.

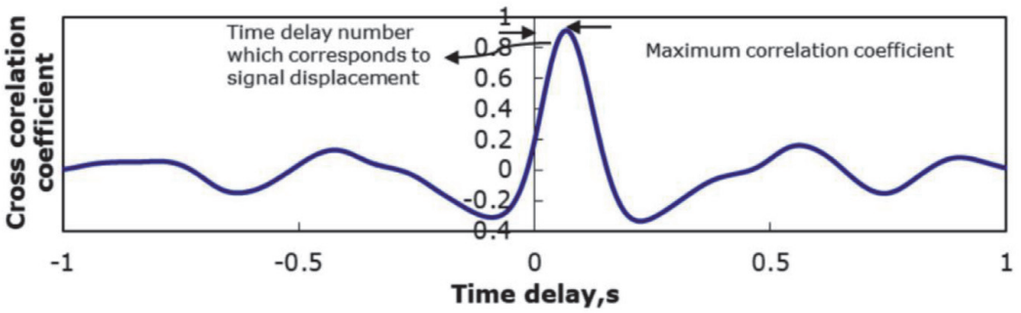

Figure 5.
Cross-correlation results for 5 mPa s silicone oil at a superficial gas velocity of 0.02 m/s.

the transit time (or time lag) which when used with the distance between the two planes leads to the calculation of the mean velocity for the slug structure.

From **Figure 5**, the y-axis on the cross-correlation plot is the correlation coefficient. This is in the range of −0.3 to +0.9 (though generally falls between −1 and +1). There could be perfect positive correlation (correlation coefficient of +1) or perfect negative correlation (correlation coefficient of −1). A positive correlation indicates that if a signal moves either up or down, the other signal will move in the same direction, while for a negative correlation, if a signal moves either up or down, the other signal will move by an equal amount in the opposite direction. When the correlation is 0, the movement of the signals gives no correlation and is completely random.

The mean velocity for the slug structure can hence be defined as distance between centres of measurement electrodes for two planes divided by the time delay [36–38].

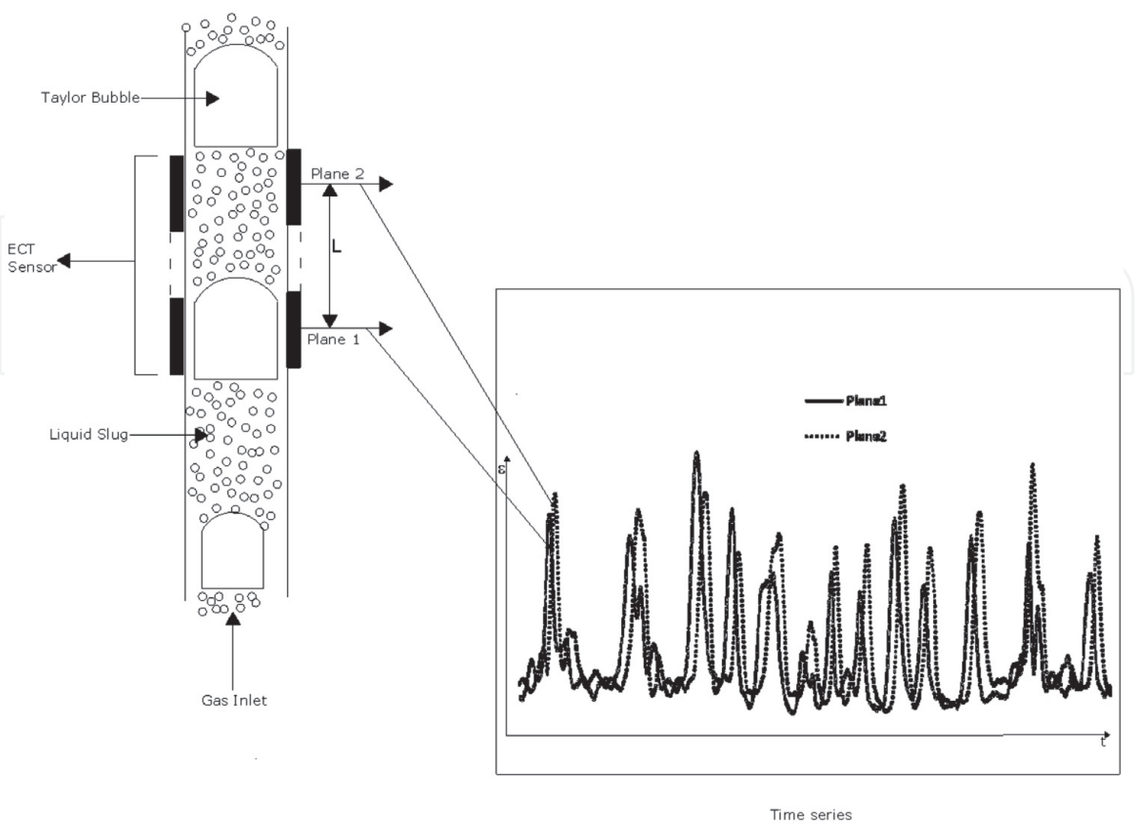

Figure 6.
ECT sensor signals generation for measurement of velocity in two-phase flows.

$$\text{Structure velocity } (\mathbf{m/s}) = \frac{\begin{matrix}\textbf{Distance between centres}\\ \textbf{of measurement}\\ \textbf{electrodes for two planes } (\mathbf{m})\end{matrix}}{\textbf{Time delay } (\mathbf{s})} \tag{22}$$

The schematics of the ECT Sensor signals generation for measurement of velocity in two-phase flows is shown in **Figure 6**.

3.2 Manual time series analysis

The structure velocity can be obtained manually by estimating the time displacement of output signals from both planes 1 and 2 via the peaks of the time series plots for both planes. Since the distance between the centres of the measurement electrodes for both planes are known, the structure velocity is hence computed using Eq. (22).

The time displacement from the time series data of both planes 1 and 2 used in the calculation of the structure velocity alongside with distance between centres of

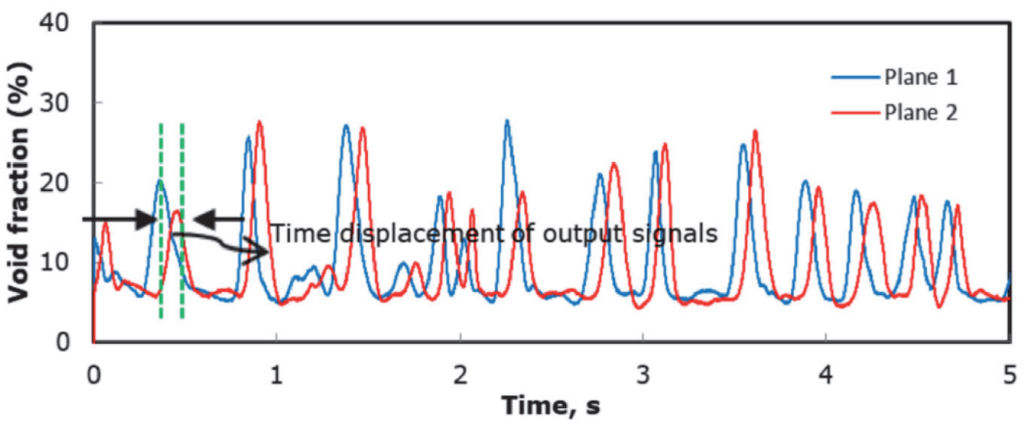

Figure 7.
Cross-sectionally averaged void fraction time series for plane 1 and 2 at a superficial gas velocity of 0.02 m/s.

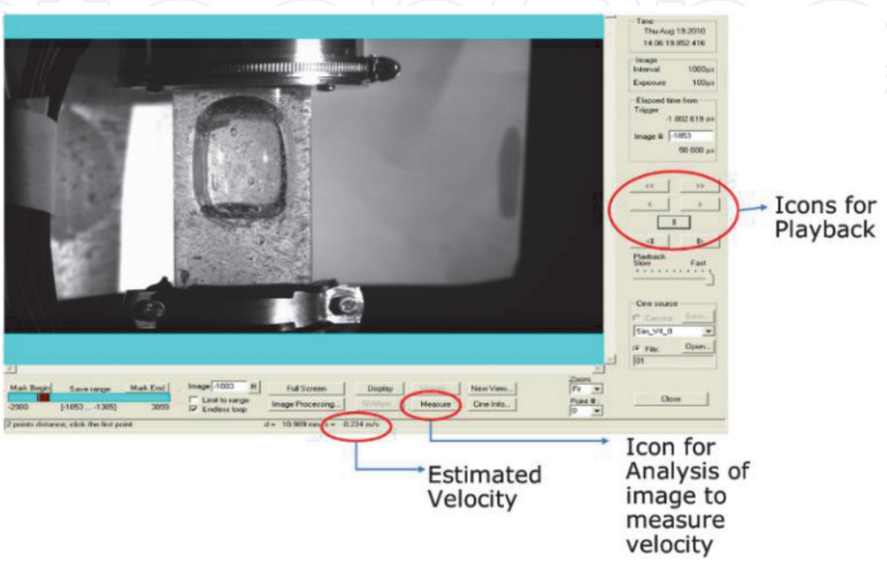

Figure 8.
Camera control software window used to estimate velocity.

measurement electrode is indicated in **Figure 7**. This is compared with that obtained via cross correlation later in this paper.

3.3 High-speed camera estimate

The camera control software of the Phantom High-Speed Camera can be used to obtain an estimate of the structure velocity. This is done via a playback in which the distance covered by the bubble at a given time is computed which gives a corresponding value for the velocity. A typical window of the camera control software is shown in **Figure 8**.

4. Results and discussion

4.1 Effect of viscosity on the rise velocity (structure velocity)

The effect of liquid viscosity on the rise velocity (structure velocity) has been studied by making a comparison between the respective structure velocities obtained from the ECT for the range of viscosities considered (i.e. 5, 100, 1000 and 5000 mPa s). The physical properties of the liquids used are given in **Table 1**.

A plot of structure velocity versus superficial gas velocity for all the viscosities considered is given in **Figure 9** which shows that structure velocity increases with an increase in superficial gas velocity which is in agreement with the observations of Abdulkaldir et al. [39] and decreases with increase in viscosity as shown in **Figure 10** (obtained from ECT Plot3d Image reconstruction software). The structure velocity of 5 and 100 mPa s is found to be approximately the same due to similar void fraction data values. The variation from small to bigger spherical cap and developing slug in 5 and 100 mPa s, and the slug flow in 1000 and 5000 mPa s (as shown in **Figure 9**) has been discussed by Kajero et al. [33].

This can be explained using the slug Reynolds number, a dimensionless parameter (Eq. 16).

A plot of slug Reynolds number versus superficial gas velocity is made at various viscosities as shown in **Figure 11**, with an indication of laminar flow.

Figure 11 reveals that as viscosity increases, slug Reynolds number decreases tending towards zero. This can be explained as follow:

i. Occurrence and prevalence of laminar flow as viscosity increases: According to Bendiksen [21], Reynolds number in the range 5000–110,000 (for low viscous fluids) give turbulent flow. As the Reynolds numbers of the viscosities considered are less than 5000, laminar flow prevails. For large slug Reynolds number, viscous effect will be negligible, while for small slug Reynolds number, viscous effect will be dominant [40]. So, since

Liquid	Viscosity, mPa s	Density, kg/m^3	Surface tension, mN/m	Relative permittivity
Silicone oil	5	915	19.7	2.60
	100	965	20.9	2.74
	1000	970	21.2	2.76
	5000	970	21.4	2.76

Table 1.
Physical properties of silicone oil viscosities used.

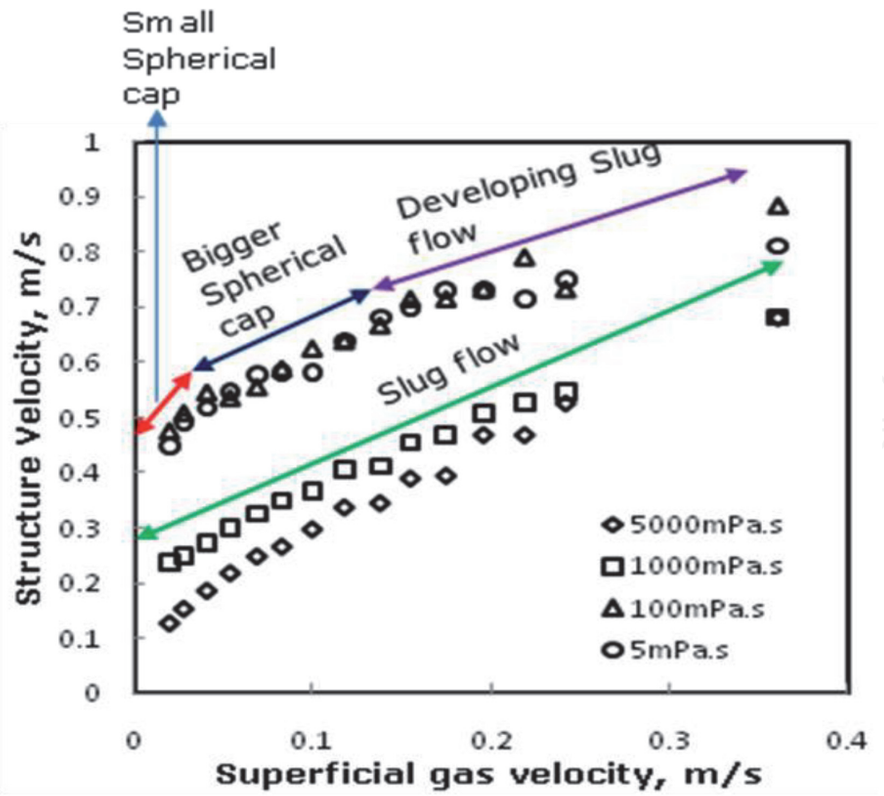

Figure 9.
Variation of structure velocity with superficial gas velocity at various viscosities.

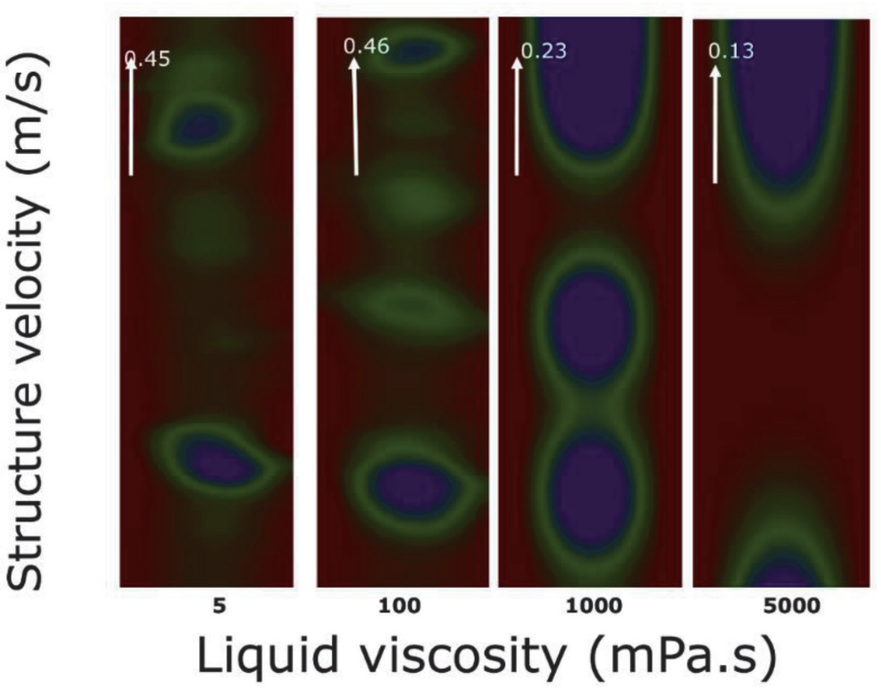

Figure 10.
Periodic structures in the slug as obtained from ECT Plot3d image reconstruction software (image display in single axial slice mode) at a superficial gas velocity of 0.02 m/s.

the slug Reynolds number for all the viscosities are small, viscous effect will be dominant.

ii. Dominating effect of viscous forces over inertia forces: Inertia forces are forces acting due to motion of bubbles through the liquid. It opposes any

force that could resist motion. Viscous forces are forces acting due to the viscous nature of the liquid. Hence, from the plot, it can be inferred that viscous forces have a domineering effect over inertia forces [41].

The forces acting on the Taylor bubble are shown in **Figure 12**. These forces have an influence on its rise velocity. Surface tension force helps to hold the bubbles together due to the cohesive force existing between them. This accounts for why 'surface tension force' was indicated at the centre of the bubble in **Figure 12**. Based on the proposition of White and Beardmore [22], the effect of surface tension force can be neglected when Eotvos number is greater than 70. So, since for all the viscosities considered, Eotvos number is greater than 70, its effect on the rise velocity of Taylor bubbles can be neglected.

The dominating effect of viscous forces over inertia forces can be further confirmed using the Inverse dimensionless viscosity according to White and Beardmore [22].

From the various viscosities considered, the dimensionless property numbers are given as follows (**Table 2**).

It will be observed that as viscosity increases, Morton number, M_o increases while the Eotvos number, E_o decreases, which culminates in the decrease of the dimensionless inverse viscosity, N_f. This confirms the proposition of Fabre and Line [42]. As the dimensionless inverse viscosity decreases, viscous effect dominates [31].

White and Beardmore [22] proposed that viscous effects come into play when the square of dimensionless inverse viscosity, N_f is less than 3×10^5. i.e.

$$(N_f)^2 = \frac{(\rho_L^2)gD^3}{\mu_L^2} < 3 \times 10^5 \tag{23}$$

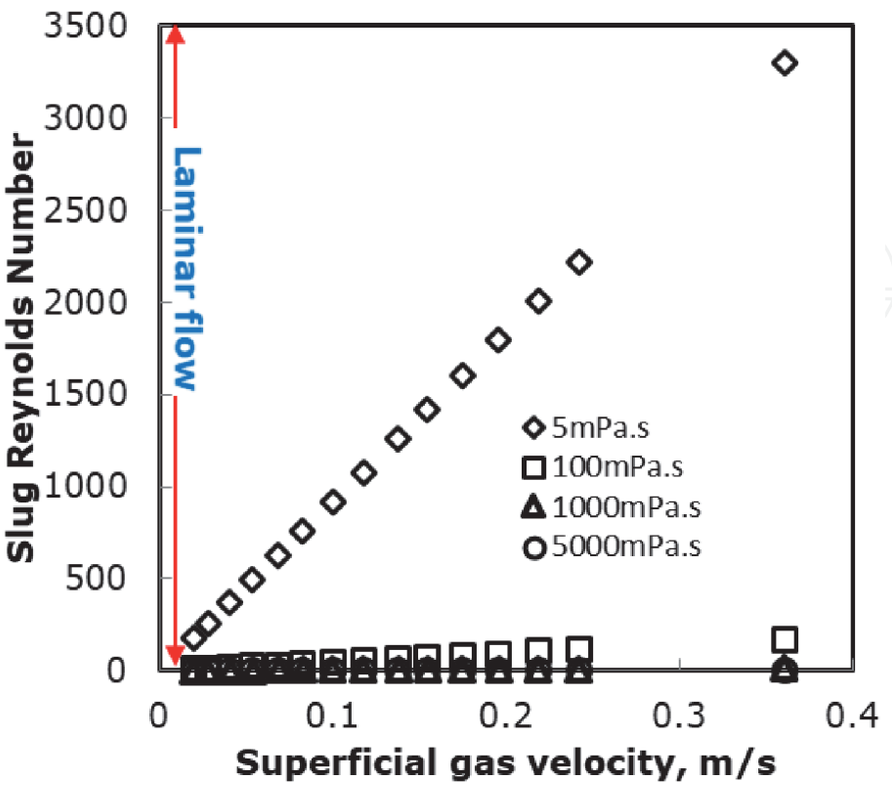

Figure 11.
Variation of slug Reynolds number with superficial gas velocity for various liquid viscosities.

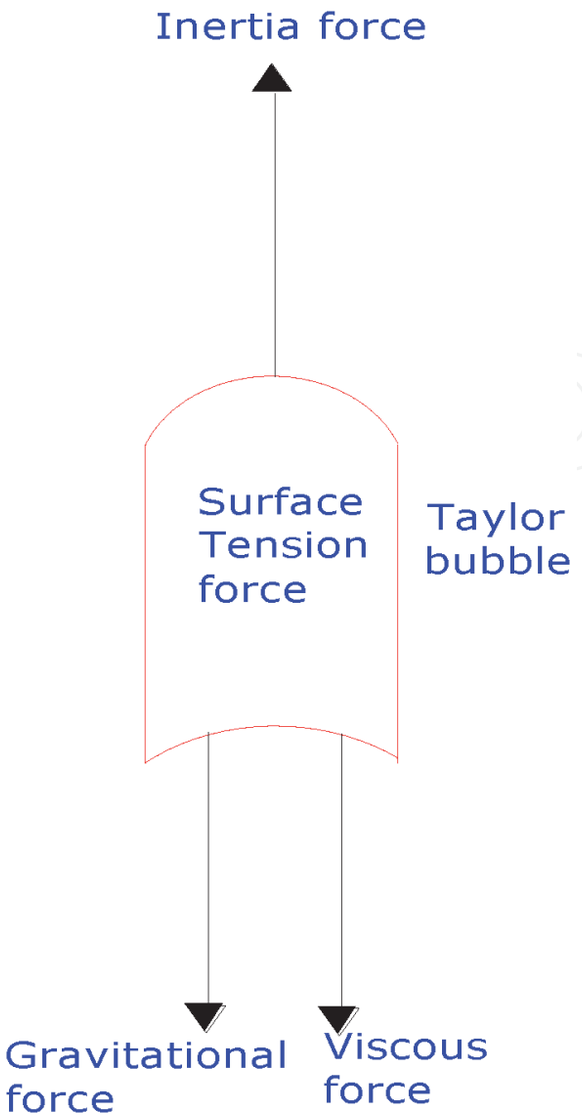

Figure 12.
Forces acting on Taylor bubble (surface tension force helps to hold the bubbles together).

Viscosity, mPa s	Dimensionless numbers		
	M_o	E_o	N_f
5	8.7645×10^{-7}	1139.105	6408.267
100	1.11353×10^{-5}	1132.374	337.9223
1000	1061.426	1122.134	33.96732
5000	644964.7	1111.647	6.793463

Table 2.
Morton, Eotvos and inverse dimensionless numbers.

The square of the inverse square dimensionless viscosity for 5, 100, 1000 and 5000 mPa s are 41,012,747, 114051.4, 1152.37 and 46.09481, respectively. Since 100 mPa s, 1000 mPa s and 5000 mPa s satisfy the condition of $(N_f)^2 < 3 \times 10^5$, viscous effect dominates. This dominating effect of viscous force over inertia force possibly causes a decrease in structure velocity with an increase in viscosity. This can be further confirmed by obtaining a relationship between drag force and viscosity taking superficial gas velocity as a parameter.

4.1.1 Drag force, F_D

From Stokes law, drag force is given as:

$$F_D = 3\pi\mu_L Vd \tag{24}$$

based on the fact that the flow is laminar.

Drag force is the force due to the resistance provided by the fluid to the motion of a body through it.

From Eq. (24), Drag force is directly proportional to viscosity of the fluid.

Drag coefficient, C_D is given as:

$$C_D = \frac{24}{Re} \tag{25}$$

On substituting Eq. (25) into (24) given that $Re = \rho_L Vd/\mu_L$,

$$F_D = \frac{72\pi\mu_L^2}{C_D\rho_L} \tag{26}$$

Eq. (26) is used to compute drag force, F_D which is plotted against superficial gas velocity for all viscosities considered as shown in **Figure 13(a)**. This can be interpreted as follows:

i. Drag force is directly proportional to viscosity, which confirms Eq. (26) according to Stokes law. Drag force is the force due to the resistance provided by the viscous nature of the silicone oil fluids to the motion of the large bubble through them. So, as viscosity increases, there is a linear increase in drag force.

ii. The increase in drag force shows an opposition to the motion of the bubbles through the liquid acting parallel to direction of relative motion, hence causing the bubbles to rise at much slower rate. This obviously leads to a decrease in the rise velocity [42].

To further confirm the effect of drag force, drag force was plotted against void fraction, which is the volume fraction of gas in the gas–liquid mixture as shown in **Figure 13(b)**.

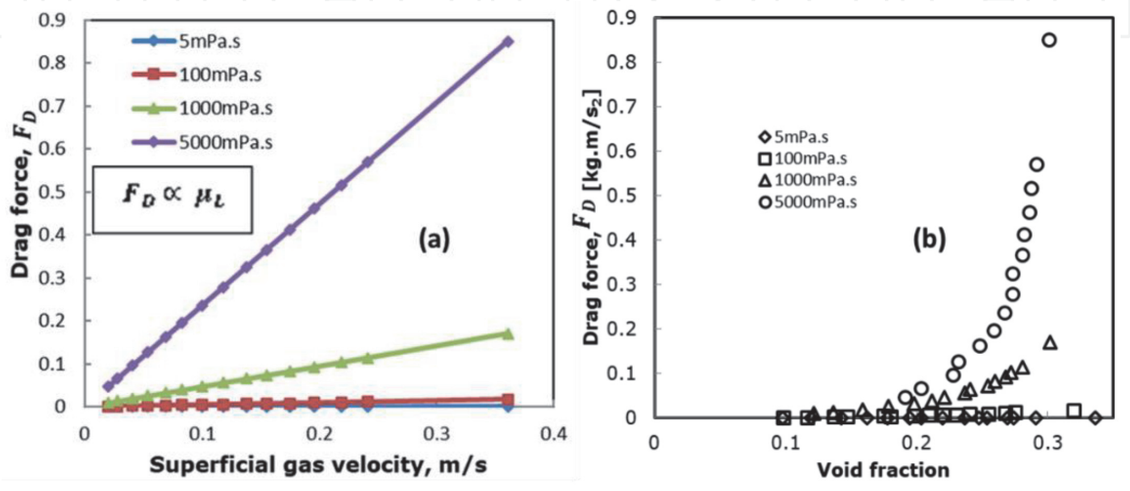

Figure 13.
Drag force versus (a) superficial gas velocity, (b) void fraction.

As void fraction increases, the drag force increases. This is probably due to the increase in the volume fraction of gas (void fraction); hence, an increase in the bubble size relative to the column diameter. This increase in bubble size is due to coalescence and it subsequently requires an increase in drag force to be effective enough to oppose the motion of the bubbles through the liquid. Hence, it can be said that the drag force is exponentially proportional to the void fraction. The drag force was found to be low at low viscosities (5 and 100 mPa s) and increases as viscosity increases. This is due to viscous effect as explained earlier on. As viscosity increases, void fraction increases; hence, an increase in drag force subsequently leads to hindered rise velocity.

The relationship between drag force and drag coefficient is shown in **Figure 14**. As viscosity decreases, the curves of the respective viscosities are tending towards zero. As drag coefficient increases, the drag force decreases tending towards zero. This gives an inverse relationship, which fits well into a power law expression, with the inverse proportionality constant increasing with increase in viscosity as shown in **Table 3**.

A plot of drag coefficient against Reynolds number on a log–log plot agrees with Stokes law, which gives an inverse relationship between the drag coefficient and Reynolds number as shown in **Figure 15**, with purple, green, blue and red for 5, 100, 1000 and 5000 mPa s respectively. This further confirms the fact that the drag force is directly proportional to the liquid viscosity. At low Reynolds number, drag coefficient is high, while at high Reynolds number, drag coefficient is low. Hence, the structure velocity of the latter is greater than the former.

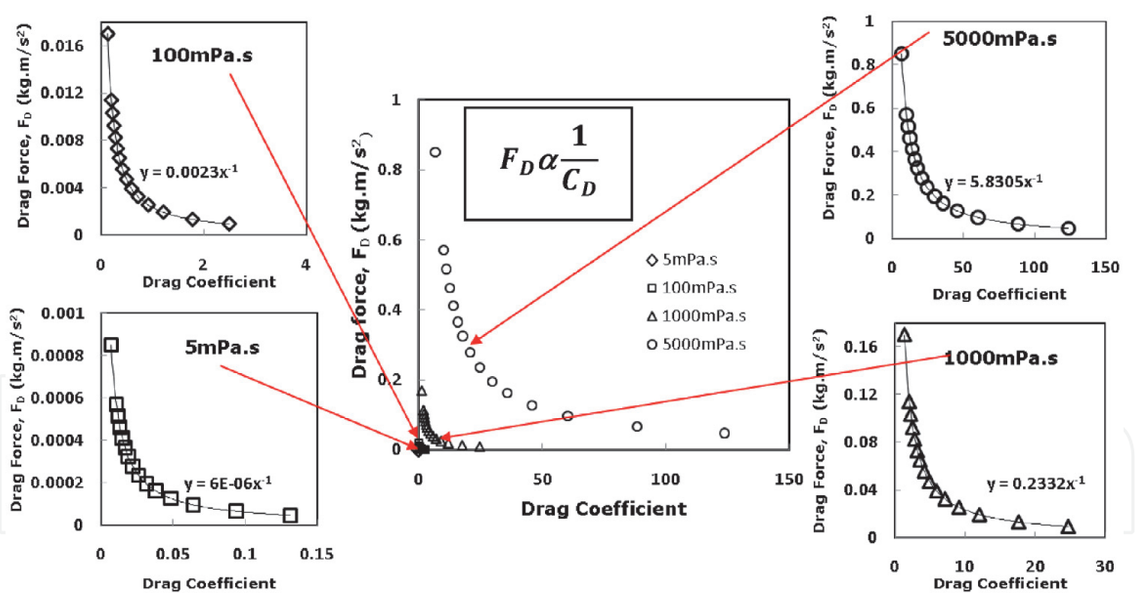

Figure 14.
Inverse relationship between drag force and drag coefficient for all the liquid viscosities considered.

Viscosity (mPa s)	Inverse proportionality constant
5	6×10^{-6}
100	0.0023
1000	0.2332
5000	5.8305

Table 3.
Inverse proportionality constants from the power law relationship between drag force and drag coefficient.

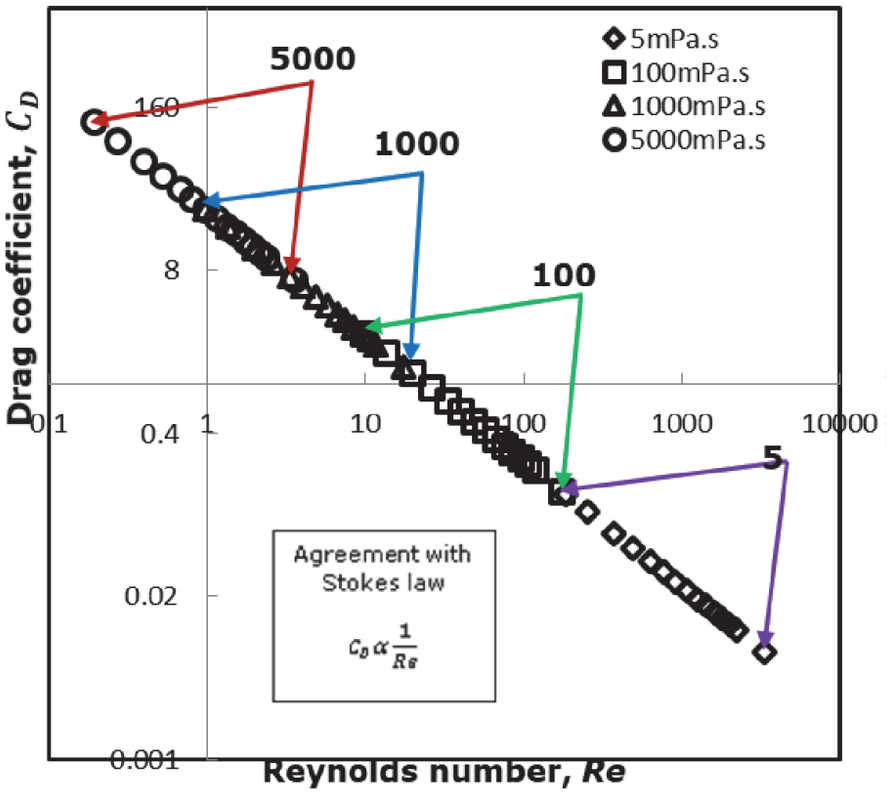

Figure 15.
Drag coefficients for the rising bubbles.

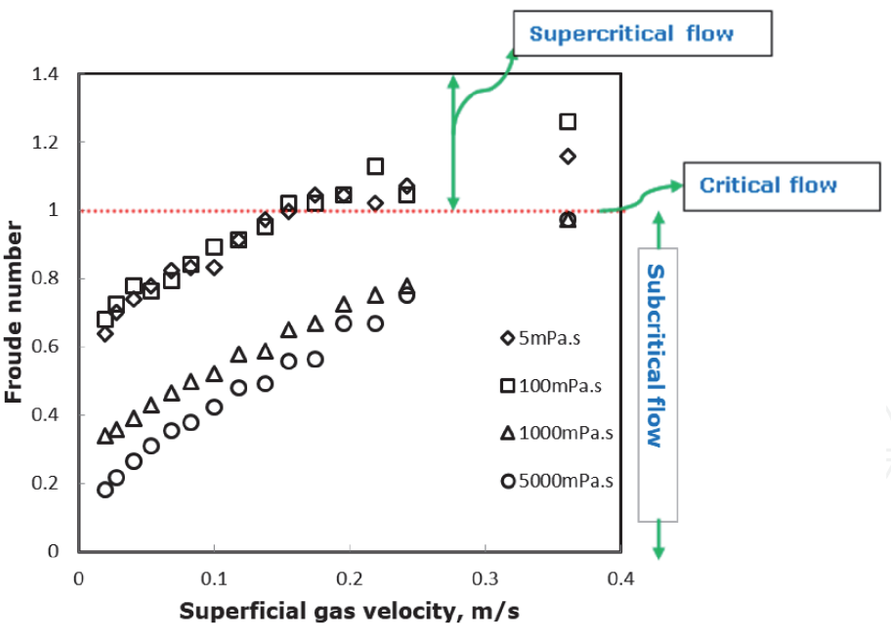

Figure 16.
Effect of Froude number.

A plot of Froude number versus the superficial gas velocity is shown in **Figure 16**. The following can be inferred from the plot:

1. At a superficial gas velocity of 0.01–0.17 m/s for both 5 and 100 mPa s viscosity, $Fr < 1$ which implies subcritical flow (slow/tranquil flow) due to low superficial gas velocity; while between 0.17 and 0.361 m/s, $Fr > 1$ which implies supercritical flow (fast rapid flow). At 0.2 m/s, $Fr = 1$ which implies critical flow [42]. In the case of both 1000 and 5000 mPa s, at all superficial

gas velocities, $Fr < 1$, this implies subcritical flow. The viscous effect makes the flow very slow, with low rise velocity of Taylor bubbles.

2. As viscosity increases, Froude number decreases which indicates the dominant effect of gravitational force over inertia force. This also has a retarding effect on the rise velocity of Taylor bubbles. Hence, this shows that the combined effect of the viscous and gravitational force causes a decrease in the rise velocity of bubbles as viscosity increases. For the high viscous liquids, 1000 and 5000 mPa s, as superficial gas velocity increases, the Froude number tends to be the same. This can be seen at 0.242 and 0.361 m/s. This implies that the dominant effect of gravitational force over inertia force tends to be the same.

4.2 Comparison of structure velocity computation methods

The structure velocity obtained from ECT was compared with the manual estimate from the time series [34], high-speed camera and empirical models such as modified Viana et al. [43], modified De Cachard and Delhaye [44], model and Nicklin et al. [7] model. These are shown in **Figure 17**.

The modified form of De Cachard and Delhaye [44] model is given as:

$$U_N = \left\{ 2.29\left[1 - \frac{20}{E_o}\left(1 - e^{-0.0125E_o}\right)\right]\right\} U_m + \Gamma\,(gD)^{1/2} \tag{27}$$

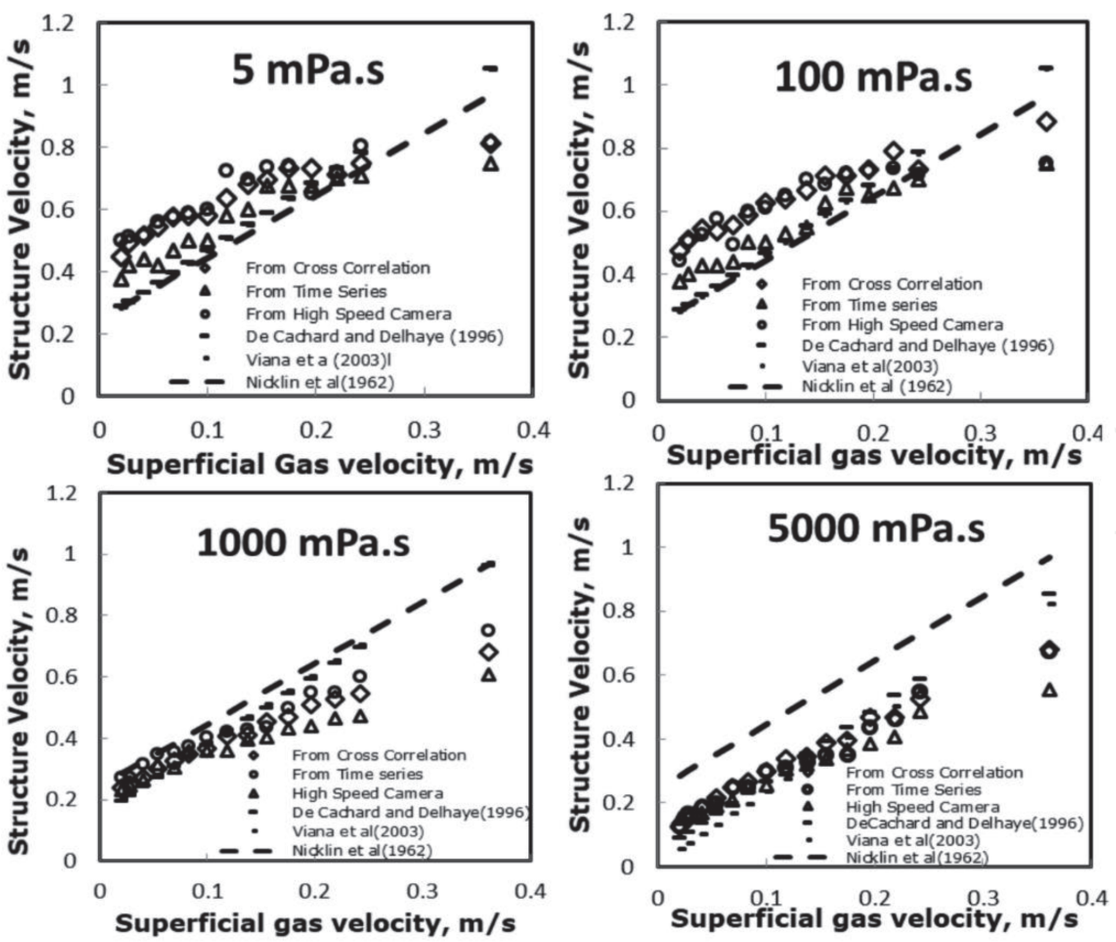

Figure 17.
Structure velocity comparison.

where Γ is given as:

$$\Gamma = 0.345\left(1 - e^{-\frac{0.01N_f}{0.345}}\right)\left[1 - e^{(3.37-B_o)/m}\right] \tag{28}$$

N_f is the inverse dimensionless viscosity.
Bond number, B_o is given as:

$$B_o = \frac{(\rho_L - \rho_G)gD^2}{\sigma} \tag{29}$$

Condition for m:

$$m = 10 \text{ when } N_f > 250 \tag{30}$$

$$m = 69(N_f)^{-0.35} \text{ when } 18 < N_f < 250 \tag{31}$$

$$m = 25 \text{ when } N_f < 18.$$

The modified form of Viana et al. [43] model is given as:

$$U_N = \left\{2.29\left[1 - \frac{20}{E_o}\left(1 - e^{-0.0125E_o}\right)\right]\right\}U_m + \sqrt[Fr]{gD} \tag{32}$$

where Fr is obtained from Eqs. (27) to (32).

$$Fr = L[R; A, B, C, G] \equiv \frac{A}{\left(1 + \left(\frac{R}{B}\right)^C\right)^G} \tag{33}$$

$$A = L[E_o; a, b, c, d] = \frac{a}{\left[1 + \left(\frac{E_o}{b}\right)^c\right]^d} \tag{34}$$

$$B = L[E_o; e, f, g, h] = \frac{e}{\left[1 + \left(\frac{E_o}{f}\right)^g\right]^h} \tag{35}$$

$$C = L[E_o; i, j, k, l] = \frac{i}{\left[1 + \left(\frac{E_o}{j}\right)^k\right]^l} \tag{36}$$

$$G = m/C \tag{37}$$

and the parameters $(a, b, \ldots \ldots \ldots, l)$ are:
$a = 0.34; b = 14.793; c = -3.06; d = 0.58; e = 31.08; f = 29.868; g = -1.96; h = -0.49; i = -1.45; j = 24.867; k = -9.93; l = -0.094; m = -1.0295.$

On the average, a good agreement exists between the structure velocity from the ECT and that measured from the high-speed camera. A reasonably fair agreement exists between the former and that estimated from the time series. The modified Viana et al. [43], modified De Cachard and Delhaye [44], and Nicklin et al. [7] model gave roughly similar pattern with structure velocity from cross-correlation, manual time series analysis and high-speed camera. Modified Viana et al. [43] and modified De Cachard and Delhaye [44] models showed good agreement with the velocity obtained from cross-correlation, manual time series analysis and

high-speed camera at low superficial gas velocity for 1000 and 5000 mPa s, while Nicklin et al. [7] over predicts it.

The variations observed in the agreement could be due to the viscosities of the liquids used. Viana et al. [43] used silicone oil of viscosity range 1–3900 mPa s. De Cachard and Delhaye [44] and Nicklin et al. [7] used water. Also, from the structure velocity plots using cross-correlation, the distribution coefficient is in the range 1.07 to 1.6, while that of modified Viana et al. [43] and De Cachard and Delhaye [44] is approximately 2.25. A distribution coefficient of 2.0 was used for Nicklin et al. [7] as proposed for laminar flow.

The video technique of determining the rise velocity of bubbles gave errors of 4.3, 4.6, 7.3 and 11.5% for 5, 100, 1000 and 5000 mPa s, respectively when compared with cross-correlation technique.

5. Conclusions

From the foregoing, the following conclusions can be drawn:

1. The forces acting on a Taylor bubble in a 50 mm column diameter include inertia force, surface tension force, viscous force and gravitational force. Surface tension force can be neglected based on Eotvos number greater than 70. The remaining forces have an influence on the rise velocity of Taylor bubble. Furthermore, viscous and gravitational forces were observed to have dominant effect over inertia forces, hence causing the rise velocity of Taylor bubbles to decrease as viscosity increases.

2. The dimensionless parameters: Froude number, Reynolds number and inverse dimensionless viscosity all played vital roles in affecting the rise velocity of Taylor bubbles in various viscosities for a 50 mm diameter column. The dimensionless parameters being functions of the fluid properties and column diameter. Froude number helped to categorize the flow in the four viscosities considered into subcritical (slow and tranquil flow, $Fr < 1$), with lower rise velocity of Taylor bubbles, critical ($Fr = 1$) and supercritical flow (fast rapid flow, $Fr > 1$), with higher rise velocity of Taylor bubbles.

3. The rise of large bubbles through the liquid in the column agrees with Stokes law where drag force is directly proportional to viscosity and an inverse relationship exists between drag coefficient and Reynolds number, as superficial gas velocity increases. The drag force is also exponentially proportional to the void fraction and it retards the motion of the Taylor bubbles through the liquid. An inverse relationship in the form of Power law expression also exists between the drag force and drag coefficient. The drag coefficient was high at low Reynolds number but low at high Reynolds number, which contributed to the rise velocity of Taylor bubbles decreasing from low to higher viscosity liquids.

4. The rise velocity of Taylor bubbles increases with an increase in superficial gas velocity for each viscosity considered (i.e. 5, 100, 1000, 5000 mPa s).

5. The comparison between the rise velocity of Taylor bubbles obtained from the ECT, high-speed camera, cross correlation, manual time series, Nickel et al. [7] model, modified models of De Cachard and Delhaye [44] and Viana et al. [43] gave reasonably fair agreement.

Dedication

This publication is in loving memory of Late Prof. Barry Azzopardi.

Nomenclature

U_N	rise velocity of Taylor bubble, m/s
μ_L	liquid viscosity, kg/m.s
D	column diameter, m
σ_L	surface tension (N/m)
ρ_L	liquid density, kg/m^3
g	acceleration due to gravity, m/s^2
U_m	mixture velocity, m/s
U_{SG}	superficial gas velocity, m/s
U_{SL}	superficial liquid velocity, m/s
Re	Reynolds number, dimensionless
E_o	Eotovos number, dimensionless
B_o	Bond number, dimensionless
Fr	Froude's number, dimensionless
M_o	Morton number, dimensionless
N_f	inverse dimensionless viscosity, dimensionless
ρ_G	gas density, kg/m^3
C_D	drag coefficient, dimensionless
F_D	drag force, N

Author details

Olumayowa T. Kajero[1*], Mukhtar Abdulkadir[2], Lokman Abdulkareem[3] and Barry James Azzopardi[4]

1 Department of Chemical and Process Engineering, University of Surrey, Guildford, United Kingdom

2 Department of Chemical Engineering, Federal University of Technology, Minna, Nigeria

3 Department of Petroleum Engineering, University of Zakho, Zakho City, Northern Iraq

4 Department of Chemical and Environmental Engineering, University of Nottingham, United Kingdom

*Address all correspondence to: ot.kajero@gmail.com

References

[1] Zukoski EE. Influence of viscosity, surface tension, and inclination angle on motion of long bubbles in closed tubes. Journal of Fluid Mechanics. 1966;**25**:821

[2] Tomiyama A, Nakahara Y, Adachi Y, Hosokawa S. Shapes and rising velocities of single bubbles rising through an inner subchannel. Journal of Nuclear Science Technology. 2003;**40**:136

[3] Mandal TK, Das G, Das PK. Prediction of rise velocity of a liquid Taylor bubble in a vertical tube. Physics of Fluids. 2007;**19**:128109

[4] Mario ART. Terminal velocity of a bubble rise in a liquid column. World Academy of Science, Engineering and Technology. 2007;**28**:264-268

[5] Llewellin EW, Bello ED, Taddeucci J, Scarlato P, Lane SJ. The thickness of the falling film of liquid around a Taylor bubble. Proceedings of the Royal Society A. 2011;**2012**(468):1041-1064

[6] Mao ZS, Dukler AE. The motion of Taylor bubbles in vertical tubes—II. Experimental data and simulations for laminar and turbulent flow. Chemical Engineering Science. 1991;**46**(8): 2055-2064

[7] Nicklin DJ, Wilkes JO, Davidson JF. Two-phase flow in vertical tubes. Transactions of the Institution of Chemical Engineers. 1962;**40**:61-68

[8] Omebere-Iyari NK, Azzopardi BJ. A study of flow patterns for gas-liquid flow in small diameter tubes. Chemical Engineering Research and Design, Institution of Chemical Engineers. 2007; **85**(A2):180-192

[9] Mao ZS, Dukler AE. The motion of Taylor bubbles in vertical tubes. I. A numerical simulation for the shape and rise velocity of Taylor bubbles in stagnant and flowing liquid. Journal of Computational Physics. November 1990;**91**(1):132-160

[10] Dumitrescu DT. Stromung an einer Luftblase im senkrechten Rohr. Zeitschrift für Angewandte Mathematik und Mechanik. 1943;**23**:139-149

[11] Davies RM, Taylor GI. The mechanics of large bubbles rising through extended liquids and through liquids in tubes. Proceedings of Royal Society London. 1949;**200**(A):375-392

[12] Griffith P, Wallis GB. Two phase slug flow. Journal of Heat Transfer. 1961;**83**:307-318

[13] Govier GW, Aziz K. The Flow of Complex Mixtures in Pipes. New York: Van Nostrand Reinhold Company; 1972

[14] Neal LG. Analysis of slip in gas-liquid flow applicable to the bubble and slug flow regimes. KR-62, Kjeller Research Establishment. Kjeller, Norway. 1963

[15] Brown RAS. Mechanics of large gas bubbles in tubes. I. Bubble velocities in stagnant liquids. Canadian Journal of Chemical Engineering. 1965;**43**:217-223

[16] Bendiksen KH, Malnes D, Nydal OJ. On the modelling of slug flow. Chemical Engineering Communication. 1996; **141–142**:71-102

[17] Collins R, De Moraes FF, Davidson JF, Harrison D. The motion of a large gas bubble rising through liquid flowing in a tube. Journal of Fluid Mechanics. 1978;**89**:497-514

[18] Bendiksen KH. On the motion of long bubbles in vertical tubes. International Journal of Multiphase Flow. 1985;**11**:797-812

[19] Douglas JR. A theoretical and experimental study of airlift pumping

and aeration with reference to agricultural applications [PhD thesis]. Cornell University; 1987

[20] Sylvester ND. A mechanistic model for two-phase vertical slug flow in pipes. ASME Journal of Energy Resources Technology. 1987;**109**:206-213

[21] Bendiksen KH. An experimental investigation of the motion of long bubbles in inclined tubes. International Journal of Multiphase Flow. 1984;**10**: 467-483

[22] White ET, Beardmore RH. The velocity of rise of single cylindrical air bubbles through liquids contained in vertical tubes. Chemical Engineering Science. 1962;**17**:351-361

[23] Morgado O, Miranda JM, Araujo JDP, Campos JBLM. Review on vertical gas-liquid slug flow. International Journal of Multiphase Flow. 2016;**85**:348-368

[24] Batchelor GK. An Introduction to Fluid Dynamics. Cambridge: Cambridge University Press; 1967. pp. 211-215

[25] Rott N. Note on the history of the Reynolds number. Annual Review of Fluid Mechanics. 1990;**22**(1):1-11

[26] Shoham O, Dukler AE. Heat transfer during intermittent/slug flow in horizontal tubes. Industrial and Engineering Chemistry Fundamentals. 1982;**21**:312-319

[27] Campos JBLM, Guedes De Carvalho JRF. An experimental study of the wake of gas slugs rising in liquids. Journal of Fluid Mechanics. 1988;**196**: 27-37

[28] Chukwu GA. Study of transportation of GTL products from Alaskan North Slope (ANS) to markets. In: Final Report. The US Department of Energy, National Energy Technology Laboratory; 2002

[29] Dukler AE, Hubbard MG. A model for gas-liquid slug flow in horizontal and near horizontal tubes. Industrial and Engineering Chemistry Fundamentals. 1975;**14**(4):337-347

[30] Lu X, Prosperetti A. A numerical study of Taylor bubbles. Industrial and Engineering Chemistry Research. 2009; **48**(1):242-252

[31] Zheng D, He X, Che D. CFD simulations of hydrodynamic characteristics in a gas-liquid vertical upward slug flow. International Journal of Heat and Mass Transfer. 2007;**50**: 4151-4165

[32] Kajero OT, Abdulkareem L, Azzopardi BJ. Effect of liquid viscosity on slug flow in a small diameter bubble column. In: Proceedings of the International Conference, Experimental Fluid Mechanics, Jicin, Czech Republic. 2011

[33] Kajero OT, Abdulkadir M, Abdulkareem L, Azzopardi BJ. Experimental study of viscous effects on flow pattern and bubble behaviour in small diameter bubble column. Physics of Fluids. 2018;**30**(9):093101

[34] Bendat J, Piersol A. Engineering Application of Correlation and Spectral Analysis. New York, USA: John Wiley and Sons; 1980

[35] Kaji R, Hills JH, Azzopardi BJ. Extracting information from the time series data in vertical upflow. Multiphase Science and Technology. 2009;**21**(1–2):185

[36] Sekoguchi K, Takeishi M, Hironaga K, Nishiura T. Velocity measurement with electrical double sensing devices in two-phase flow. In: Measuring Techniques in Gas-Liquid Two Phase Flows: Symposium. 1984. pp. 455-477

[37] Abdulkareem LA. Tomographic investigation of gas-oil flow in inclined

risers [PhD thesis]. Department of Chemical and Environmental Engineering, University of Nottingham; 2011

[38] Crowe CT. Multiphase Flow Handbook. USA: CRC Press/Taylor and Francis Group; 2006

[39] Abdulkadir M, Hernandez-Perez V, Sharaf S, Lowndes IS, Azzopardi BJ. Experimental investigation of phase distributions of an air-silicone oil flow in a vertical pipe. World Academy of Science, Engineering and Technology (WASET). 2010;**61**:52-59

[40] Robert WF, Philip JP, Alan TM. Introduction to Fluid Mechanics. 7th ed. India: John Wiley and Sons; 2010

[41] Thizon P, Contanceau M. Wall effect on the bubble behaviour in highly viscous liquids. Journal of Fluid Mechanics. 1981;**107**:339-373

[42] Fabre J, Line A. Modeling of two-phase slug flow. Annual Review of Fluid Mechanics. 1992;**24**:21-46

[43] Viana F, Pardo R, Yanez R, Trallero JL. Universal correlation for the rise velocity of long gas bubbles in round pipes. Journal of Fluid Mechanics. 2002;**494**:379-398

[44] Cachard F, Delhaye J. A slug-churn flow model for small-diameter airlift pumps. International Journal of Multiphase Flow. 1996;**22**:627-649